



Electron tomography of embedded semiconductor quantum dot

Inoue, Tomoya

Kita, Takashi

Wada, Osamu

(Citation)

Applied Physics Letters, 92(3):031902-031902

(Issue Date)

2008-01-23

(Resource Type)

journal article

(Version)

Version of Record

(URL)

<https://hdl.handle.net/20.500.14094/90000742>



Electron tomography of embedded semiconductor quantum dot

Tomoya Inoue, Takashi Kita,^{a)} and Osamu Wada

*Department of Electrical and Electronics Engineering, Faculty of Engineering, Kobe University,
1-1 Rokkodai, Nada, Kobe 657-8501, Japan*

Mitsuru Konno, Toshie Yaguchi, and Takeo Kamino

*Nanotechnology Products Business Group, Hitachi High-Technologies Corporation, 1-1 Ishikawa,
Hitachinaka, Ibaraki 312-0057, Japan*

(Received 3 September 2007; accepted 4 January 2008; published online 23 January 2008)

We performed an electron tomography for a single InAs quantum dot (QD) embedded in GaAs. A comprehensive three-dimensional image of indium distribution has been reconstructed by using a high-angle annular dark-field scanning transmission electron microscope. This was achieved by using a special nanopillar specimen prepared by a focused ion beam technique. The real structure of the embedded single QD has been found to have a complicated anisotropic structure reflecting the QD structure before being capped. © 2008 American Institute of Physics.

[DOI: [10.1063/1.2837453](https://doi.org/10.1063/1.2837453)]

Ultranarrow excitonic transitions in a semiconductor quantum dots (QDs) are attracting strong interest for applying to quantum information processing devices such as a source of event-ready polarization entangled photon pairs.¹ Especially, InAs QDs have been widely studied because of the operation in the infrared optical communication bands. Since the exciton fine structure of the QD is modified by electron hole exchange interactions, in-plane asymmetries of the structural properties lift the degeneracy of the intermediate exciton states in the biexcitonic system, which eventually gives rise to the “which path” information. Generally, it is believed that the InAs QD is elongated along the $[-110]$ crystal axis.² However, there is no direct evidence of a real InAs QD embedded in GaAs, where atomic segregation effects must modify the as-deposited QD structure. Therefore, a comprehensive understanding of the precise three-dimensional (3D) structure of the QD becomes a key issue in order to understand the fine exciton states in a single QD and control the optical properties completely.

Recently, a cross-sectional scanning-tunneling microscopy (STM) has been used to investigate a single InAs QD structure embedded in GaAs and clear indium segregation from the QD into the capping layer has been found.³ However, the QD structure in the STM image depends on the cleaved plane and it is impossible to reconstruct the complete 3D structure. In contrast to this, transmission electron microscopy (TEM) is the most powerful and direct method to observe the crystallographic structure of the embedded QD. The conventional TEM image, however, is a projection of the 3D object on a two-dimensional (2D) screen. To obtain detailed 3D information of a single QD, we have conceptually advanced the TEM technology by combining with the focused ion beam (FIB)-microsampling technique and anisotropic structural properties of a single InAs QD embedded in GaAs has been confirmed.⁴ However, the large lattice mismatch (7%) of InAs/GaAs causes substantial strain-field contrast in the TEM image. Thereby, as the strain extends further out of the QD into the surrounding material, a zone-axis orientation with lots of strain contrast show a larger

structure. To avoid such strain effects in the highly strained system of InAs/GaAs QDs, high-angle annular dark-field scanning transmission electron microscope (HAADF-STEM) is known to be a powerful technique.⁵ The HAADF-STEM visualizes the atomic number contrast (Z contrast). Here, we performed reconstruction of the 3D image of InAs QD from HAADF-STEM images taken from multidirections by using a specimen prepared by the FIB-microsampling method.^{4,6} The processed pillar specimen enables one to rotate completely 360° and avoid variations in the sampling thickness depending on the incident beam direction. Using a series of tilted Z-contrast images, strain-free 3D images of crystalline nanostructures can be reconstructed,^{7,8} which is called HAADF-STEM tomography.

Self-assembled InAs QDs were grown on a GaAs(001) substrate by solid-source molecular beam epitaxy system. QDs can be formed naturally by the Stranski-Krastanov growth-mode transition from the 2D growth to the 3D island growth. After growing a 500 nm buffer layer of GaAs at 550 °C, InAs was deposited at 460 °C and the nominal thickness was 3.6 ML. Above the critical thickness of 1.8 ML, the transition from the 2D wetting layer growth to the 3D island growth spontaneously occurs owing to the large lattice mismatch between InAs and GaAs. Finally, the sample was capped by a 150 nm thick GaAs layer at 460 °C.

A TEM specimen was fabricated by the FIB-microsampling technique using a recently developed FIB/STEM compatible specimen rotation holder. First, a small piece of a specimen was cut out from an epitaxial wafer. Then, the extracted specimen was fixed onto the end of the specimen rotation holder. After milling to a size of $\sim 300 \times 300 \text{ nm}^2$, we selected a single QD for the observation by HAADF-STEM. In order to extract the single QD, the pillar was reduced to about $140 \times 140 \text{ nm}^2$. During the process, the pillar was monitored by STEM. Finally, a damaged layer surrounding the pillar, which is caused by the FIB process, was removed by using a low-energy (500 eV) Ar-ion milling. As a result of this gentle milling, the pillar size was reduced to a diameter of 75 nm.

We carried out the HAADF-STEM observation by using Hitachi HD2700 STEM equipped with an aberration-

^{a)}Electronic mail: kita@eedept.kobe-u.ac.jp.

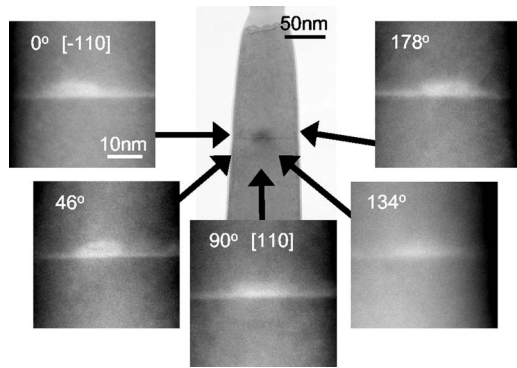


FIG. 1. Nanopillar specimen and typical HAADF-STEM images recorded at multidirections. Specimen was milled to a diameter of 75 nm. HAADF-STEM images were recorded every 2° from 0° to 178° with rotating specimen around the $[001]$ axis. Corresponding HAADF-STEM images are arranged in around the pillar.

corrected objective lens. The acceleration voltage was 200 kV. The electron beam diameter was 0.2 nm and the range of the collection angle was in the range of 80–350 mrad. HAADF-STEM images were recorded every 2° from 0° to 178° with rotating specimen around the $[001]$ axis. From a series of the rotated HAADF-STEM images, we reconstructed a tomography image.

A bright field TEM image of the nanopillar specimen is shown at the center in Fig. 1. The selected single QD is confirmed to be placed at the center of the pillar sample. Some of many HAADF-STEM images are arranged in around the pillar. Since the HAADF-STEM contrast directly relates to the atomic number, the obtained image represents distribution of indium atoms integrated along the electron-beam incident direction.

A bird's eye view of a tomography image reconstructed from these HAADF-STEM images taken from multidirections is displayed in Fig. 2. The computed brightness is considered to obey a linear dependence on the local indium content because we have not applied any nonlinear image corrections such as gamma correction. The single QD is found on the thin wetting layer clearly. It is noted that the contrast of the GaAs capping layer just above the wetting layer is found to become bright. This indicates that indium atoms segregate during the growth from the wetting layer into the GaAs capping layer.

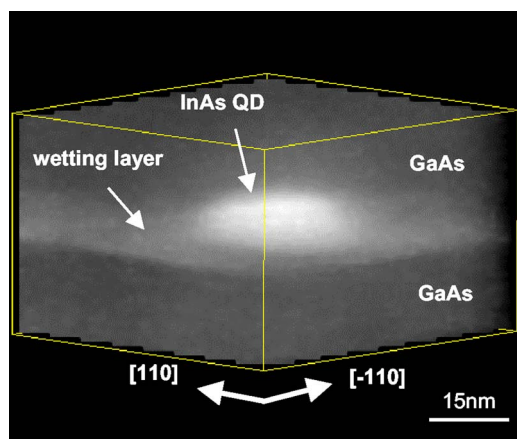


FIG. 2. (Color online) A bird's eye view of the reconstructed tomography image.

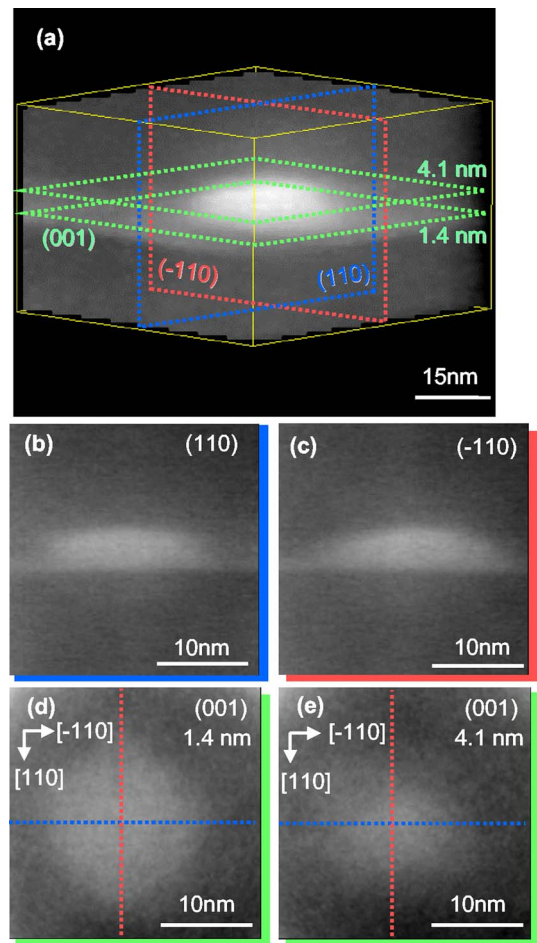


FIG. 3. (Color online) Tomography image and 2D cross-section images of an embedded single InAs quantum dot. (a) 3D tomography image. [(b) and (c)] 2D mappings of the indium concentration of (110) and (-110) cross sections including the center of the QD as indicated by dotted blue and red lines in (a), respectively. The (110) cross section (b) shows a flat interface between the dot and the capping layer, while the (-110) cross section (c) shows a round interface between them. [(d) and (e)] (001) cross section images sliced at 1.4 and 4.1 nm from the base of the QD as indicated by dotted green lines in (a), respectively. The structure near the base (d) shows a round square. The shape near the top (e) shows a sort of a rugby ball shape elongated along the $[-110]$.

Next, we analyze 2D cross sections of this 3D reconstruction. The results are summarized in Fig. 3. Figures 3(b) and 3(c) show the (110) and (-110) cross-section images of the indium distribution as indicated by dotted blue and red lines in Fig. 3(a), respectively. Both the cross sections include the center of the QD. The QD silhouette in the (110) cross section is found to have a flattened topmost interface between the QD and the GaAs capping layer, while the top in the (-110) cross section shows a round shape. Figures 3(d) and 3(e) show the (001) cross-section images sliced at the height of 1.4 and 4.1 nm from the base of the QD, respectively. The structure near the base of the QD, Fig. 3(d), has been revealed to be a round square shape. However, the in-plane cross-section image at 4.1 nm from the base shows a sort of a rugby ball shape elongated along the $[-110]$, as shown in Fig. 3(e). Therefore, the embedded QD is concluded to be an island with twofold symmetry on the base with fourfold symmetry.

Here, we compare the results with a typical model of uncapped QDs studied by the STM.⁹ Generally, it is well known that an uncapped QD is surrounded by $\{137\}$, $\{011\}$, AIP license or copyright; see <http://apl.aip.org/apl/copyright.jsp>

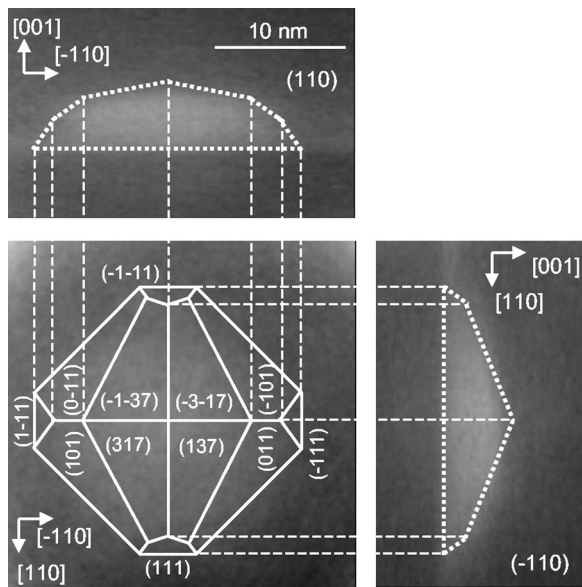


FIG. 4. Comparison between the present tomography image and an ideally faceted model structure which is cited from Ref. 9. In the model, QD structure is assumed to consist of $\{137\}$, $\{011\}$, and $\{111\}$ planes.

and $\{111\}$.⁹ As illustrated in Fig. 4, in spite of the obscure image, the observed structure moderately agrees with a frame consisting of the $\{137\}$, $\{011\}$, and $\{111\}$ facets except for the apex. The diffuse interface and the truncated apex are considered to be typical characteristics caused by indium segregation during the capping layer deposition.¹⁰ In spite of this shape modification, it is noted that the anisotropic structure appears in the capped QD according to the anisotropic faceted structure of the as-deposited QD.

In summary, we have demonstrated a complicated anisotropic QD island structure using HAADF-STEM tomogra-

phy with a specimen prepared by the FIB-microsampling method. The QD can be viewed from multidirections and a conclusive and comprehensible determination of the size and shape anisotropy has been realized. The 3D tomography demonstrated that a flattened topmost interface of the QD along the $[-110]$ direction, while the interface along $[110]$ shows a round shape. Furthermore, it was found that the embedded QD is an island with twofold symmetry on the base with fourfold symmetry. Such detailed structural information, which has never been observed, is believed to provide important insights for optimizing growth strategies to produce QD with fully isotropic shape enabling the emission of entangled photon pair. Here, we have to emphasize that the combined use of the FIB-microsampling technique and HAADF-STEM tomography is applicable to any material systems and even to complicated device structures.

¹R. M. Stevenson, R. J. Young, P. Atkinson, K. Cooper, D. A. Ritchie, and A. J. Shields, *Nature (London)* **439**, 179 (2006).

²B. A. Joyce and D. D. Vvedensky, *Mater. Sci. Eng., R.* **46**, 127 (2004).

³D. M. Bruls, J. W. A. M. Vugs, P. M. Koenraad, H. W. M. Salemink, J. H. Wolter, M. Hopkinson, M. S. Skolnick, F. Long, and S. P. A. Gill, *Appl. Phys. Lett.* **81**, 1708 (2002).

⁴T. Kita, T. Inoue, O. Wada, M. Konno, T. Yaguchi, and T. Kamino, *Appl. Phys. Lett.* **90**, 041911 (2007).

⁵P. Wang, A. L. Bleloch, M. Falke, P. J. Goodhew, J. Ng, and M. Missous, *Appl. Phys. Lett.* **89**, 072111 (2006).

⁶T. Kamino, T. Yaguchi, M. Konno, T. Ohnishi, and T. Ishitani, *J. Electron Microsc.* **53**, 583 (2004).

⁷P. A. Midgley and M. Weyland, *Ultramicroscopy* **96**, 413 (2003).

⁸I. Arslan, T. J. V. Yates, N. D. Browning, and P. A. Midgley, *Science* **309**, 2195 (2005).

⁹M. C. Xu, Y. Temko, T. Suzuki, and K. Jacobi, *J. Appl. Phys.* **98**, 083525 (2005).

¹⁰G. Costantini, A. Rastelli, C. Manzano, P. Acosta-Diaz, R. Songmuang, G. Katsaros, O. G. Schmidt, and K. Kern, *Phys. Rev. Lett.* **96**, 226106 (2006).